Decadal Variability in the Impact of Atmospheric Circulation Patterns on the Winter Climate of Northern Russia

GARETH J. MARSHALL[a]

[a] *British Antarctic Survey, Cambridge, United Kingdom*

(Manuscript received 21 July 2020, in final form 13 October 2020)

ABSTRACT: The Arctic continues to warm at a much faster rate than the global average. One process contributing to ''Arctic amplification'' involves changes in low-frequency macroscale atmospheric circulation patterns and their consequent influence on regional climate. Here, using ERA5 data, we examine decadal changes in the impact of seven such patterns on winter near-surface temperature (SAT) and precipitation (PPN) in northern Russia and calculate the temporal consistency of any statistically significant relationships. We demonstrate that the 40-yr climatology hides considerable decadal variability in the spatial extent of such circulation pattern–climate relationships across the region, with few areas where their temporal consistency exceeds 60%. This is primarily a response to the pronounced decadal expansion/contraction and/or mobility of the circulation patterns' centers of action. The North Atlantic Oscillation (NAO) is the dominant pattern (having the highest temporal consistency) affecting SAT west of the Urals. Farther east, the Scandinavian (SCA), Polar/Eurasian (POL), and West Pacific patterns are successively the dominant pattern influencing SAT across the West Siberian Plains, Central Siberian Plateau, and mountains of Far East Siberia, respectively. From west to east, the SCA, POL, and Pacific–North American patterns exert the most consistent decadal influence on PPN. The only temporally invariant significant decadal relationships occur between the NAO and SAT and the SCA and PPN in small areas of the North European Plain.

KEYWORDS: Arctic; Atmospheric circulation; Teleconnections; Climate variability; Decadal variability

1. Introduction

The climate of the northern high latitudes is changing faster than elsewhere. Recent warming in near-surface Arctic temperatures has been more than twice that at lower latitudes (e.g., Overland et al. 2016), a phenomenon termed Arctic amplification. Moreover, regional precipitation has also increased (e.g., Box et al. 2019). Both changes have been at least partially ascribed to anthropogenic forcing (e.g., Chylek et al. 2014; Min et al. 2008). A significant proportion of the terrestrial Arctic comprises northern Russia, which stretches more than 7000 km from ~30°E eastward to ~170°W (Fig. 1). This region has the potential to exert a huge influence on future greenhouse gas emissions because of the substantial amounts of carbon stored in its wetlands, soil, boreal forest, and terrestrial and shelf seas permafrost (e.g., Groisman et al. 2017, and references therein; Vasiliev et al. 2020). Many of these carbon sinks can only exist as such within narrow temperature ranges and are especially vulnerable to the ongoing warming, which was particularly marked across much of Siberia during the first half of 2020 (World Weather Attribution 2020).

Therefore, it is imperative to understand the multiple processes that contribute to Arctic climate change, not least because of the divergent conclusions of studies assessing the impact of Arctic amplification on severe winter weather in midlatitudes (e.g., Cohen et al. 2020, and references therein). One such process concerns changes in the atmospheric circulation at northern high latitudes, which alters the spatial distribution of wind-induced heat advection and precipitation-bearing clouds with associated regional changes in the radiation budget (Ye et al. 2015). Much of the low-frequency, macroscale atmospheric variability can be expressed as a series of atmospheric circulation (or teleconnection) patterns, which describe anomalous circulation conditions that occur simultaneously over remote regions. The locations of the maximum anomalies, usually defined in a pressure or geopotential height field, are termed ''centers of action,'' with their sign reversing between the opposite phases (or polarities) of the pattern. The majority of these circulation patterns are associated with large-scale changes in the atmospheric wave and jet stream patterns, and the centers of action appear as ''standing'' waves or north–south-oriented dipoles (e.g., Handorf and Dethloff 2012). They are driven primarily by either internal atmospheric dynamics or atmosphere–ocean–ice interactions, both of which can be modified by external anthropogenic forcing. These circulation patterns are generally more prevalent and have centers of action of greater magnitude during the

Denotes content that is immediately available upon publication as open access.

Supplemental information related to this paper is available at the Journals Online website: https://doi.org/10.1175/JCLI-D-20-0566.s1.

Corresponding author: Gareth J. Marshall, gjma@bas.ac.uk

DOI: 10.1175/JCLI-D-20-0566.1

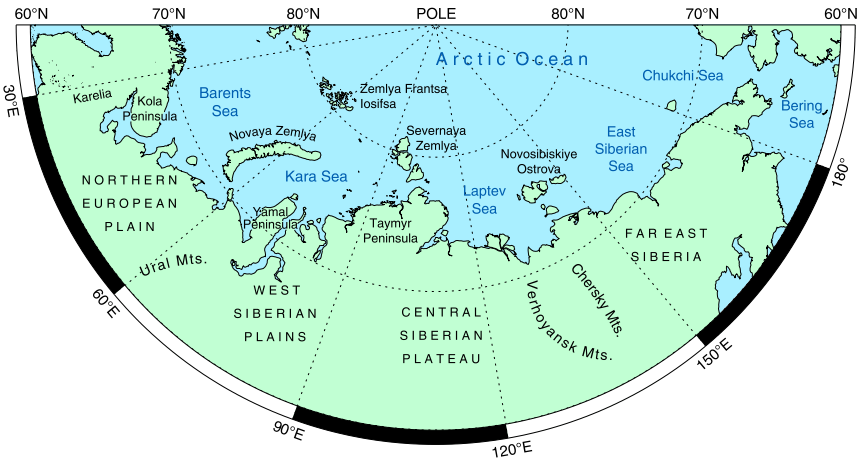

FIG. 1. Map of northern Russia and surrounding marginal seas, showing places mentioned in the text.

boreal winter, and thus engender a larger impact on climate variability in this season.

While these patterns may be considered as a continuum rather than discrete regimes (Franzke and Feldstein 2005), they are more usually described as separate entities following their definition in the pioneering work of Wallace and Gutzler (1981) and Barnston and Livezey (1987). The vast expanse of northern Russia means that its climate is shaped by circulation patterns originating in several oceanic basins: the North Atlantic Oscillation (NAO), East Atlantic pattern (EA), East Atlantic/Western Russia pattern (EAWR), and Scandinavian pattern (SCA) in the North Atlantic, the West Pacific pattern (WP) and Pacific–North American pattern (PNA) in the North Pacific, and the Polar/Eurasian pattern (POL) over the Arctic basin. Summary details of these seven circulation patterns are provided in Table 1. There is a large body of scientific research examining the impact of the North Atlantic and North Pacific patterns on the climate of western Europe and North America, respectively: however, there are far fewer examples in the western literature that investigate their influence on Eurasia including northern Russia. We note that while an alternative atmospheric catalogue (the Vangengeim–Girs classification) is sometimes employed in Russia and eastern Europe—see Degirmendžić and Kożuchowski (2019) for a description and recent use of this classification—there are marked similarities between this and many of the atmospheric circulation patterns listed above (Hoy et al. 2013; Gao et al. 2016).

TABLE 1. Summary details of the circulation patterns examined in this study.

Circulation pattern	Acronym	Boreal winter centers of action relevant for this study (signs for positive polarity)	References
North Atlantic Oscillation	NAO	North–south dipole: Greenland/Iceland (−) and the Azores (+)	Barnston and Livezey (1987) Hurrell (1995)
East Atlantic	EA	North–south dipole: across the North Atlantic, generally displaced southeast from NAO pattern	Barnston and Livezey (1987)
West Pacific	WP	North–south dipole: Kamchatka Peninsula (−) and Southeast Asia/western subtropical North Pacific (+)	Wallace and Gutzler (1981) Barnston and Livezey (1987)
Pacific– North American	PNA	Standing wave: intermountain region of North America (+) and south of Aleutian Islands (−)	Barnston and Livezey (1987)
East Atlantic/Western Russia	EAWR (Eurasia-2)	Standing wave: western Europe (+), north of Caspian Sea (−), northern China (+)	Barnston and Livezey (1987) Lim (2015)
Scandinavian	SCA (Eurasia-1)	Standing wave: western Europe (−), Scandinavia (+), eastern Russia (−)	Barnston and Livezey (1987) Bueh and Nakamura (2007)
Polar/Eurasia	POL	North–south dipole: Arctic Ocean (−) and northern China (+)	Climate Prediction Center (https://www.cpc.ncep.noaa.gov/data/teledoc/poleur.shtml)

A positive NAO generally favors warmer and wetter conditions over much of northern Russia (e.g., Hurrell 1995; Hurrell et al. 2003; Shmakin and Popova 2006; Bader et al. 2011). For example, a positive winter NAO is usually associated with southerly flow over the far northwest of the region (e.g., Kislov and Matveeva 2020), leading to a warmer and wetter Kola Peninsula (Marshall et al. 2016), and is a major impact on winter climate extremes in this area (Casanueva et al. 2014; Marshall et al. 2020). Popova (2007) documented a negative relationship between the NAO and snow depth in northwest Russia because in mild winters precipitation is more likely to fall as rain. Other studies have analyzed the effects of the Arctic Oscillation (AO), which is broadly analogous to the NAO, and shown similar climatic relationships (e.g., Frey and Smith 2003; Yu et al. 2017). Previous work has also revealed that variability in autumn Eurasian snow cover, Arctic sea ice extent, North Atlantic sea surface temperature, and regional atmospheric circulation anomalies can feed back onto the subsequent winter NAO/AO (e.g., Chen et al. 2020; Cohen et al. 2020; Henderson et al. 2018; Kryjov 2015; Wu et al. 2013). The EA and EAWR patterns affect the intensity of the winter westerly wind belt over Eurasia (Gao et al. 2016). The positive polarity of the EAWR is associated with warming over eastern Siberia and has a wavelike appearance consistent with its wave train structure (Liu et al. 2014). It has also been linked to above average precipitation in the West Siberian Plains and the Kola Peninsula (Ionita 2014; Lim 2015). During the positive phase of the winter SCA most of Eurasia north of 40°N is colder than normal (Liu et al. 2014), with an increase in the frequency of extreme cold events (Yu et al. 2017). Decreased precipitation occurs over northwestern Russia, the West Siberian Plains, and some of the Arctic coastal region, associated with reduced storm-track activity (Bueh and Nakamura 2007; Popova 2007; Liu et al. 2014). Crasemann et al. (2017) established that a positive winter SCA was more likely to occur following reduced Arctic sea ice in the preceding autumn although Peings (2019) found that blocking in this region was associated with internal variability rather than regional sea ice anomalies. There have been especially few studies regarding the effects of the North Pacific patterns—WP and PNA—and POL on Russian climate. Popova (2007) demonstrated an increase (decrease) in snow depth in the West Siberian Plains (the Far East region of Siberia) related to both positive PNA and POL. Interestingly, she also noted significant negative snow depth anomalies in the Kola Peninsula linked to the WP, despite this pattern having a center of action thousands of kilometers away in the North Pacific.

The majority of these previous studies have examined the climatological (long-term average) influence of circulation patterns on northern Russian climate over several decades. However, it is known that in addition to the relative frequency of the positive and negative polarities of a pattern varying through time (e.g., Hanna et al. 2015), the locations of the centers of action of these patterns are not temporally invariant and therefore neither is the spatial distribution of their climatic impacts (e.g., Goosse and Holland 2005; Vicente-Serrano and López-Moreno 2008; Zhang et al. 2008). The strength of the relationship between the circulation patterns and their proposed drivers (or statistical predictors) within the climate system may also be nonstationary, perhaps in response to changes in the background state (e.g., Kolstad and Screen 2019). Popova (2018) described decadal-scale variability in the climatic impact of the patterns in the north of Eurasia linked to switches in the rate of global warming. Moreover, modeling studies suggest that as the Arctic warms further the links between the dominant circulation patterns and Arctic surface climate are likely to vary considerably (van der Linden et al. 2017). Thus, in order to improve estimates of uncertainty in future climate projections it is important to understand how the climatic impacts of these atmospheric circulation patterns vary at decadal time scales and longer during the recent past. In this study we provide the first detailed analysis of the decadal variability in the influence of seven circulation patterns on the winter climate of northern Russia: such decadal-scale variability may be hidden in correlations calculated over longer time periods. Specifically, we examine seasonal gridded near-surface air temperature (SAT) and precipitation (PPN) reanalysis data over the past four decades. Changes in these two parameters can have significant consequences: for example, disrupting fragile natural Arctic terrestrial ecosystems (Cooper 2014) and causing devastating socioeconomic impacts for indigenous peoples dependent on tundra reindeer nomadism (Forbes et al. 2016).

In section 2 we describe the data and statistical methodologies employed. In presenting the results (section 3) we 1) define the average circulation pattern–climate relationships for the past 40 years; 2) as examples of decadal variability, examine how these vary across four successive decades in response to changing locations of the centers of action; 3) summarize the temporal consistency of statistically significant decadal relationships and determine which circulation patterns are most temporally consistent with SAT and/or PPN across different regions of northern Russia; and 4) extend the length of the analysis using an alternative gridded climate dataset. Finally, in section 5, we summarize our principal conclusions, and discuss them in the context of previous and proposed future work.

2. Data and statistical methods

a. Climate data

We utilize monthly SAT and PPN data from ERA5, the latest European Centre for Medium-Range Weather Forecasts (ECMWF) reanalysis, which is currently available from 1979 to the present. Seasonal winter values were simply calculated as the mean of the December–February monthly values for 1980–2019 where the year refers to the January. ERA5 has both higher spatial and temporal resolution than its predecessors: 31 km and hourly, respectively. In combination with improved modeling of surface conditions and more consistent sea surface temperature and sea ice analyses, this helps give improved SAT in the Arctic (Hersbach et al. 2020). Moreover, precipitation over Arctic sea ice was found to be more representative of the limited observations than earlier reanalyses (C. Wang et al. 2019).

To extend the length of our analysis and test the robustness of the results we use the Japanese Meteorological Agency

(JMA) 55-year Reanalysis (JRA-55) (Kobayashi et al. 2015), for which data are available from 1958 to the present. The spatial resolution of JRA-55 is approximately half that of ERA5, at ~55 km, and the monthly SAT (PPN) data are the mean of four daily 6-h analyses (forecasts). Importantly, Marshall et al. (2018) found that JRA-55 reproduced the climate of Arctic Fennoscandia with a similarly high accuracy across its whole time series.

Time series of the seven atmospheric circulation patterns—the NAO, EA, WP, PNA, EAWR, SCA, and POL—were obtained from the National Weather Service Climate Prediction Center (CPC), where the methodology for calculating them, as employed by Barnston and Livezey (1987), is also described. In short, rotated principal component analysis was used to identify the patterns based on monthly mean standardized 500-hPa height anomalies derived from the NCEP–NCAR reanalysis (Kalnay et al. 1996) in the region 20°–90°N for 1950–2000. An examination of the 12 calendar monthly sets of rotated modes of variability revealed 10 dominant circulation patterns, of which seven are analyzed here. Although some of these patterns only explain a small proportion of the total variance in the height fields, previous work has indicated they are all physically meaningful at seasonal frequencies (Barnston and Livezey 1987). The sign conventions of some of the patterns vary between different past studies: here we use those of the CPC. We note that the North Pacific Oscillation (NPO) may be considered to be the surface manifestation of the WP (Linkin and Nigam 2008) but here we use the CPC WP index as it is compatible with the time series of the other circulation patterns. We also note that the exact impact a circulation pattern has on regional climate may be dependent on how it is defined (e.g., Pokorná and Huth 2015). Of particular relevance to this study, Chen and Song (2018) demonstrated that the effect of the NPO (similar to the WP) on winter SAT in parts of Far East Siberia varied by several degrees Celsius across six definitions.

Seasonal winter indices were calculated in the same way as the seasonal reanalysis data. We do not include the Arctic Oscillation (Thompson and Wallace 1998) because it is highly correlated to the NAO ($r = 0.75$ for the 40 winters examined here) and has a broadly similar impact on climate across northern Russia, although with slightly weaker (stronger) relationships in the west (east) of the region. To clarify, in this study we investigate how the climatic impacts of the atmospheric circulation patterns, rather than the patterns themselves, vary at decadal time scales.

b. Statistical methods

All regression and correlation analyses were undertaken on detrended time series, thus assuming no a priori link between the two datasets. Regression coefficients were calculated using standard least squares methodology and the statistical significance obtained using Student's t test. In the latter calculation, we assumed there is no correlation between successive winter values of the circulation patterns or meteorological data (e.g., Feldstein 2002). In addition, we employed the Brown–Forsythe test for the equality of variances (Brown and Forsythe 1974) and the false discovery rate test, as described in Wilks (2006).

3. Results

a. Climatological winter relationships

To set the decadal variability of the influence of each of the different atmospheric circulation patterns on the winter climate of northern Russia in context, first we describe the mean climatological relationships for the 40 years from 1980 to 2019. In Fig. 2 we show the spatial pattern of the regression coefficients between each of the positive polarities of the circulation patterns and sea level pressure (SLP)—the contour spacing of which is analogous to the associated near-surface wind anomalies—and the regions where a significant relationship ($p < 0.10$) exists between the pattern and SAT and PPN. Note that circumpolar plots to 50°N of the regression coefficients are provided in Fig. S1 in the online supplemental material, which enable that fraction of the spatial pattern over northern Russia to be set in the context of the full pattern. The relatively high spatial resolution of ERA5 allows us to detect the impact that major orographic barriers, such as the Urals, have on these relationships.

1) North Atlantic Oscillation

The NAO center of action in the region is the northeast extension of the Icelandic low that stretches north of Fennoscandia (Fig. 2i). The resultant cyclonic circulation for positive NAO (NAO+) leads to anomalous southwesterly flow over northwestern Russia, bringing warmer, moist air from the south. The widespread impact of the NAO on SAT in northern Russia is clearly indicated in Fig. 2ii, with a significant positive relationship between the two across almost all land north of 60°N and west of 130°E. The positive relationship between PPN and NAO across northwest Russia is less spatially coherent (Fig. 2iii): nevertheless, there is still a significant relationship between the NAO and PPN across the majority of land west of 90°E. The rain-shadow effect of the Urals at ~60°E can be perceived by the lack of a significant relationship between the NAO and PPN on the lee (east) side.

2) East Atlantic

EA+ has a center of action over the Arctic Ocean giving anticyclonic flow over much of northern Russia in combination with negative centers of action farther south (Fig. 2iv). The easterly circulation anomaly over the Arctic coast leads to significantly colder SAT in this region between 45°–120°E, including Novaya Zemlya and Severnaya Zemlya (Fig. 2v). EA+ is also associated with significant decreases in PPN over parts of the same region together with smaller areas of increased PPN farther south, immediately east of the Urals—in contrast to NAO+ the locally anomalous easterly flow associated with EA+ means that the rain-shadow effect of the Urals is observed on the western side—and in parts of the Central Siberian Plateau (~100°E) (Fig. 2vi).

3) West Pacific

The negative northern center of action of WP+ is located over the Bering Sea (Fig. 2vii), which gives weak northeasterly circulation anomalies in Far East Siberia. While WP+ is linked to significantly colder SAT over the mountains of eastern

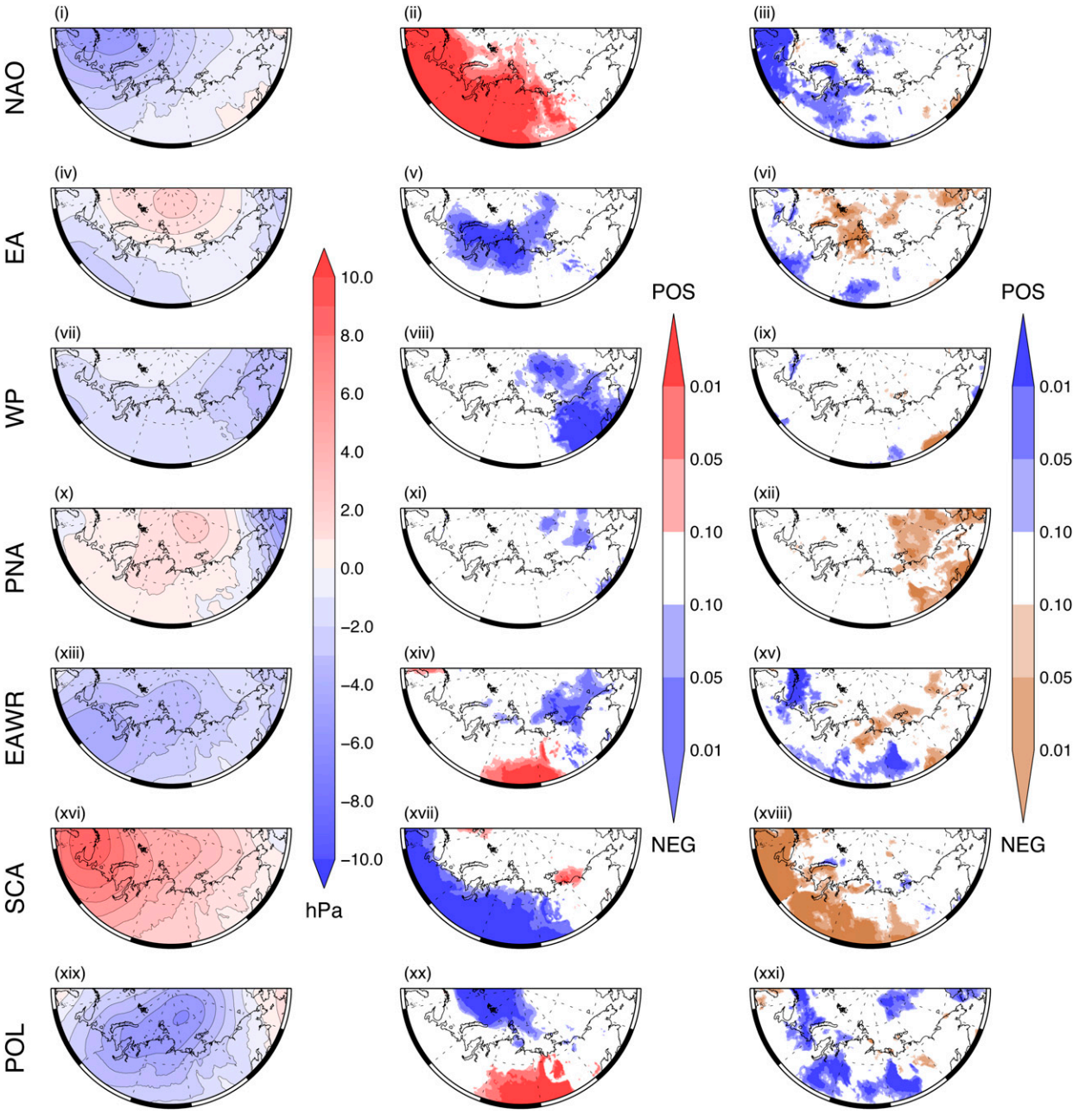

FIG. 2. (left) The spatial pattern of the regression coefficients between the positive polarity of the circulation patterns and SLP, and the statistical significance between the positive polarity of the pattern and (center) SAT and (right) PPN. Analysis is based on 40 years of ERA5 winter data (1980–2019, where the year refers to the January).

Siberia (Fig. 2viii), there are no large coherent areas of anomalous PPN in northern Russia associated with this circulation pattern (Fig. 2ix).

4) PACIFIC–NORTH AMERICA

Similar to WP+, PNA+ also has a negative center of action in the North Pacific. However, Fig. 2x reveals that the northerly wind anomalies are much greater than for WP+ (contours closer together). There is also a positive center of action over the Arctic Ocean, north of the Laptev Sea, which means that the anomalous circulation associated with PNA+ over northern Russia is confined to the far east of the region. In contrast to WP+, PNA+ has very little impact on regional SAT (Fig. 2xi) but is concomitant with significantly reduced PPN over parts of Far East Siberia (Fig. 2xii).

5) EAST ATLANTIC/WESTERN RUSSIA

The winter EAWR+ pattern comprises four centers of action, one of which can be observed in Fig. 2xiii, with two of the others in Fig. S1v in the online supplemental material. This is a

broad negative SLP anomaly, centered north of the Caspian Sea (~60°E), which gives anomalous northerly flow over the Barents Sea and weaker southwesterly flow across much of northern Russia east of 90°E. The associated winter SAT anomalies are warmer (colder) in parts of the Central Siberian Plateau (the East Siberian Sea) (Fig. 2xiv). The latter observation is noteworthy because one might expect the anomalously southerly flow associated with EAWR+ to give warmer SAT: it arises because the climatological winter temperature over the East Siberian Sea is warmer than the region of Far East Siberia to the south. The stronger northerly flow over the Barents Sea during EAWR+ gives greater PPN over the northern Kola Peninsula (Fig. 2xv). There are also areas of significant changes in PPN of both signs in the Central Siberian Plateau associated with EAWR+, with increases generally found farther south, matching the regions of anomalous warming.

6) SCANDINAVIAN

The SCA pattern has a primary center of action over the Kola Peninsula, which, as the CPC defines the SCA, is a positive SLP anomaly for SCA+ (Fig. 2xvi). Therefore, the resultant anticyclonic circulation causes anomalous northerly flow into northern Russia immediately to the east, over the Kara Sea. Given that the climatological SLP regression patterns of NAO+ and SCA+ are almost opposite in spatial extent (cf. Figs. 2i and 2xvi), it is not surprising that their associated climatic anomalies also generally ''mirror'' each other. Thus, there are significant negative SAT anomalies across most of northern Russia west of 130°E (Fig. 2xvii). Interestingly, in contrast to the NAO, the impact of the SCA on SAT does not extend as far north as the Arctic coast in parts of this region, such as the Kola, Yamal, and Taymyr Peninsulas. However, the region of significant decreases in PPN accompanying SCA+ is larger and more spatially coherent than the equivalent increases associated with NAO+ (cf. Figs. 2iii and 2xviii).

7) POLAR/EURASIA

The principal regional center of action of the POL+ pattern comprises a broad negative anomaly centered over the Kara and Laptev Seas (Fig. 2xix), analogous to an intensified polar vortex in the Eastern Hemisphere. This circulation pattern leads to a more zonally directed flow at ~65°N that inhibits meridional exchanges of heat and moisture between the Arctic and midlatitudes. Significant SAT anomalies linked to POL+ therefore form a north–south dipole, with colder (warmer) temperatures over the Arctic Ocean, including Zemlya Frantsa Iosifa (Central Siberian Plateau) (Fig. 2xx). Almost all the associated PPN anomalies are positive and although such areas are scattered across much of northern Russia, including the Barents Sea coast and parts of western and central Siberia, they are sufficiently large in extent to signify they are not simply noise (Fig. 2xxi).

b. Variability across successive decades

In this section we use four successive decades—1980–89, 1990–99, 2000–09, and 2010–19—as independent examples of the decadal variability of the impact of the seven atmospheric circulation patterns on the winter climate of northern Russia. Plots of the significant relationships between the positive polarities of the patterns and SAT and PPN are shown in Figs. 3 and 4, respectively, with equivalent plots of the regression coefficient provided in Figs. S2 and S3, respectively. while the seasonal regression between the patterns and SLP is shown in Fig. 5. The temporal variability of significant ($p < 0.10$) decadal pattern–climate relationships in different regions between the four decades (simply defined as when the majority of the region has such a relationship) is summarized in Fig. 6.

Figures 3 and 4 reveal that there is indeed very marked decadal variability in the spatial locations and extent over which an individual circulation pattern exerts a statistically significant influence on the climate of northern Russia. This is despite there often being concomitant long-term ''climatological'' relationships over the same 40-yr period (cf. Fig. 2). Figure 6 demonstrates that there was not a single statistically significant ''regional-scale'' relationship between a circulation pattern and either SAT or PPN that occurred across all four decades. Some decadal differences are especially striking: for example, the change in spatial extent of the significant impact of the NAO between the 1980s and 1990s (cf. Figs. 3i and 4i and Figs. 3ii and 4ii). There are also some instances of reversals in the sign of significant regional-scale relationships, such as between the PNA and SAT in Far East Siberia in the 2000s and 2010s (cf. Figs. 3xv and 3xvi). Figures 3 and 4 indicate that the areas where there is a significant relationship at $p < 0.10$ but not at $p < 0.05$ are generally very small. Therefore, the results in Fig. 6 are not substantially dependent on using the lower significance level. However, there are one or two exceptions, such as the relationship between WP and SAT over the Northern European Plain during the 2000s (Fig. 4xi) and that between EAWR and PPN over the West Siberian Plains in the same decade (Fig. 5xix).

Examination of Fig. 5 suggests that a high proportion of the decadal variability is likely to be a direct response to the changing location and/or extent of a pattern's center(s) of action, which modifies the spatial distribution of advection of heat and moisture into and across the region. In the 1980s the NAO center of action north of Fennoscandia, the Icelandic low, expanded farther east than average, as far as the Laptev Sea (Fig. 5i), whereas during the 1990s the center of action retracted back westward (Fig. 5ii); broadly similar eastward extents of the Icelandic low were observed in the 2000s and 2010s, respectively (Figs. 5iii and iv). The SCA and PNA also display comparable decadal variability in the extent of their principal centers of action, situated in the west (Figs. 5xxi–xxiv) and east (Figs. 5xiii–xvi) of northern Russia, respectively. The principal regional center of action of both the EAWR and POL patterns was present in all four decades, but its location exhibited considerable variability (Figs. 5xvii–xx and 5xxv–xxviii, respectively). Moreover, in the case of the EA and WP patterns, there were changes in both the sign and location of the associated centers of action over northern Russia (Figs. 5v–viii and 5ix–xii).

Another potential source for the differences between the impact of the atmospheric circulation patterns in the four successive decades is that the pattern itself is dominated by

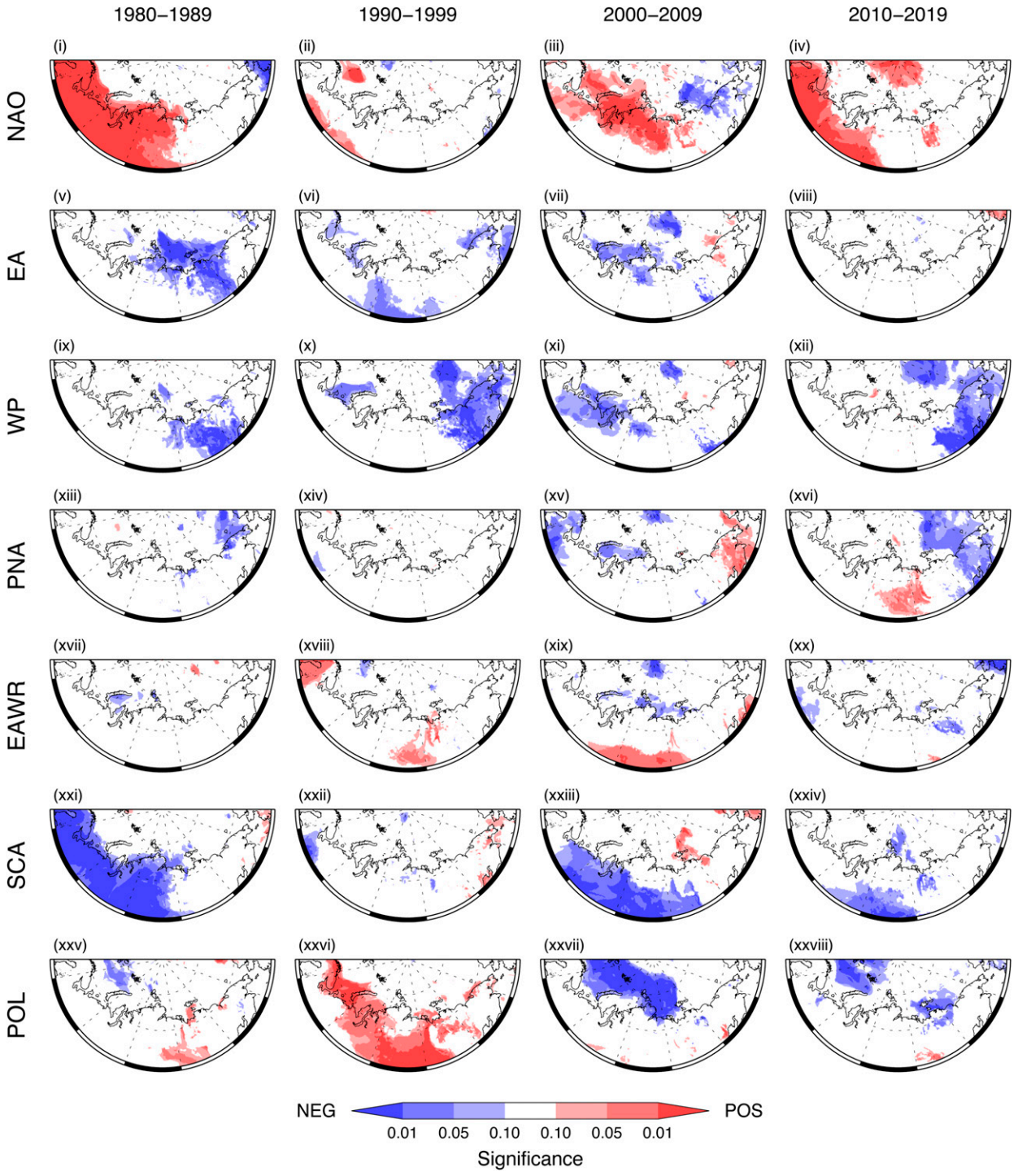

FIG. 3. The spatial pattern of the statistical significance between the positive polarity of the circulation patterns and SAT for the 1980s, 1990s, 2000s, and 2010s. Analysis is based on ERA5 winter data, and the year refers to the January.

decadal variability. For example, if in a given decade the polarity remained positive then the shape of its distribution would be different from a decade when the polarity varied across both signs, and thus we could expect differences in the regression coefficient for a given significance level. To address this issue, we compare the variance of the four successive decades against the climatology using the Brown–Forsythe test (Brown and Forsythe 1974). This reveals that none of the circulation patterns has a variability in any of the four decades that is significantly different from the climatology ($p < 0.10$). Moreover, if

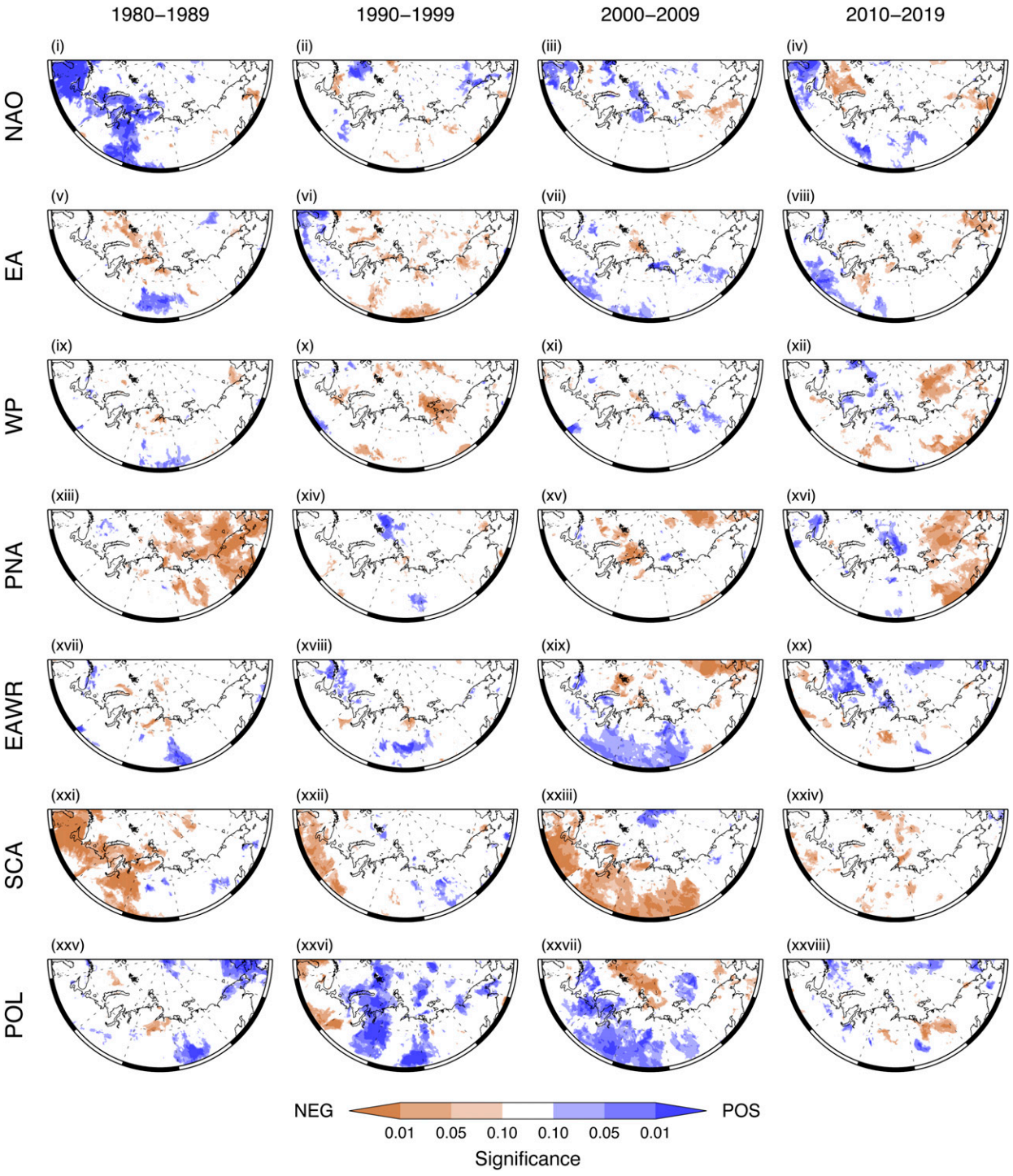

FIG. 4. As in Fig. 3, but showing the statistical significance between the positive polarity of the circulation patterns and PPN.

we examine the regression coefficients (Figs. S2 and S3) we can see that they broadly follow the significance levels. For instance, the magnitude of the regression coefficients between the NAO and SAT are much higher over the Northern European Plain and West Siberian Plains in the 1980s (>4°C), when there was a significant relationship, than in the following decade when there was not (<2°C) (cf. Figs. S2i and Fig. S2ii). Thus, we conclude that decadal changes in climate–circulation pattern relationships across northern Russia result predominantly from decadal changes in the anomalous circulation associated with that pattern.

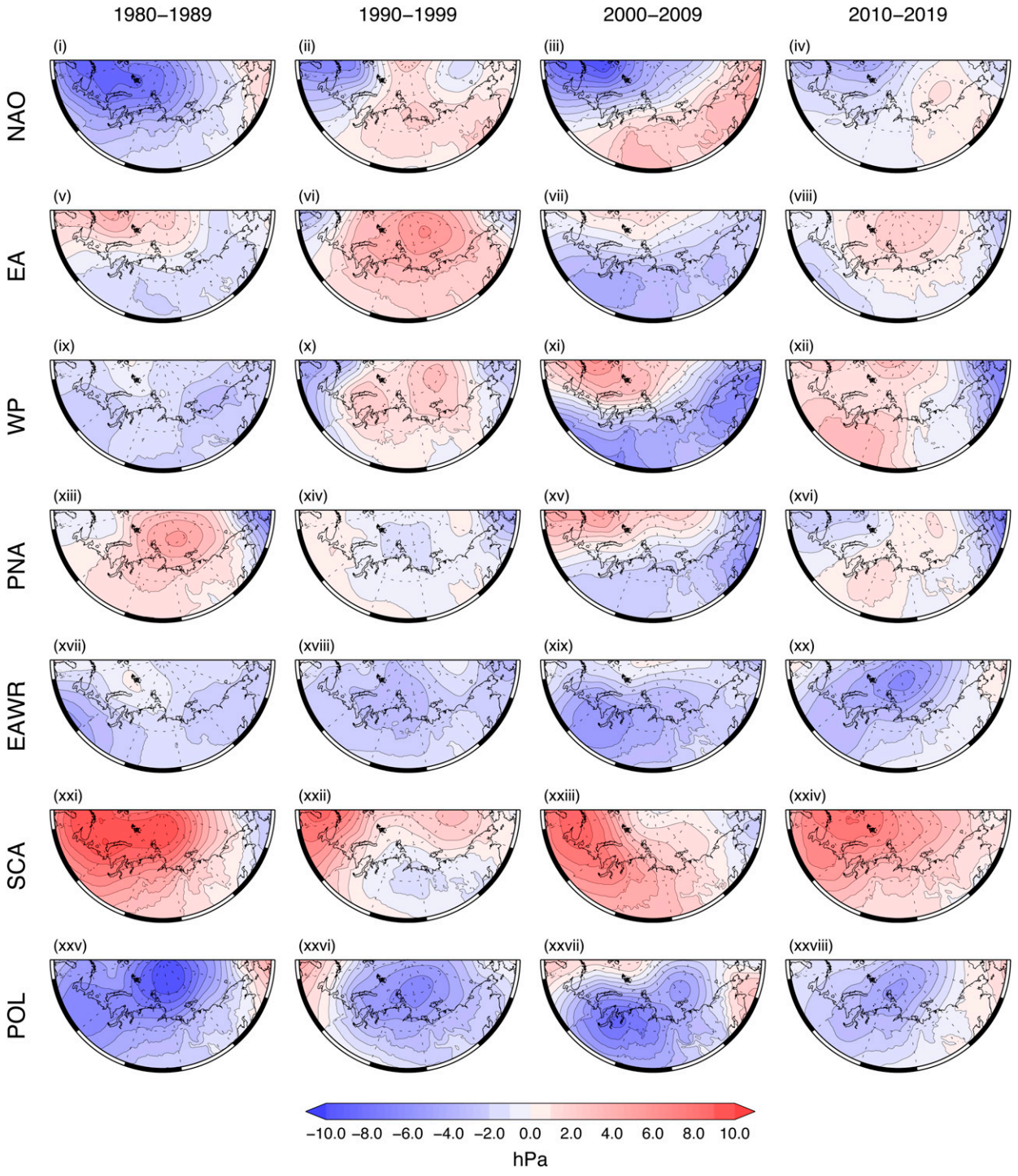

FIG. 5. As in Fig. 3, but showing the regression coefficients between the positive polarities of the circulation patterns and SLP.

c. Decadal variability of the spatial impact of the circulation patterns

As a measure of this variability, we next examine the spatial patterns of temporal consistency. This is simply a measure of the probability that a statistically significant correlation between an atmospheric circulation pattern and SAT or PPN occurs in an arbitrary decade. Maps of the temporal consistency, derived from the 31 decades within the 1980–2019 period and using a significance level of $p < 0.10$, are shown in Fig. 7. Thus, if a significant correlation occurs in 20 of these 31 decades at a location, then the temporal consistency of the relationship there is

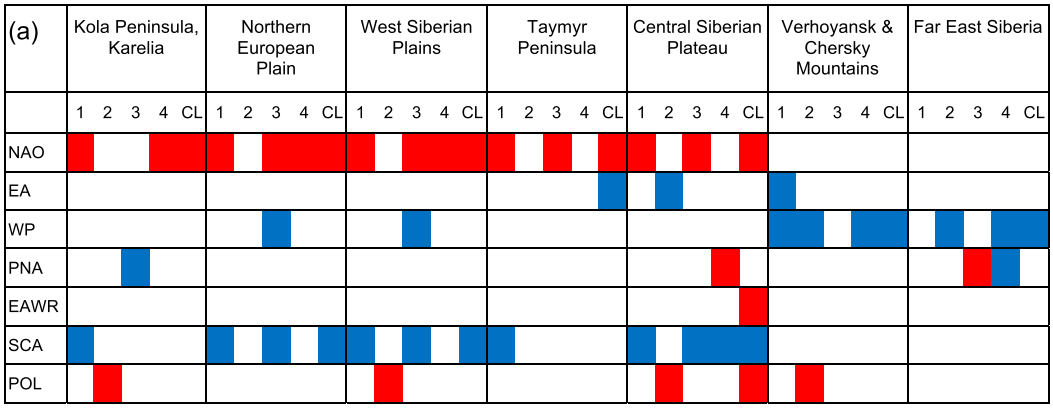

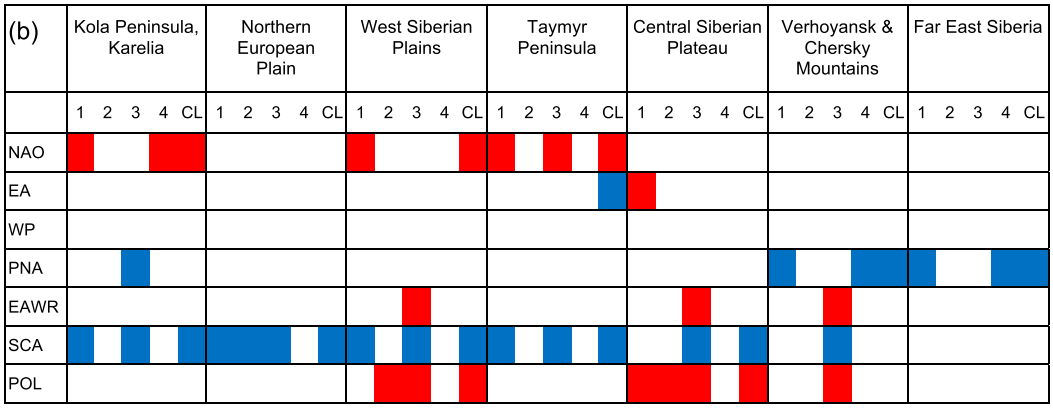

FIG. 6. Summary of the spatial distribution of significant winter decadal relationships ($p < 0.10$) in four consecutive decades—1) 1980s, 2) 1990s, 3) 2000s, and 4) 2010s—between the circulation patterns and (a) SAT and (b) PPN across selected regions of northern Russia (cf. Fig. 1). Red and blue indicate a significant positive and negative relationship, respectively, while white indicates no significant relationship in that decade.

~65%. Note that when significant circulations of both signs occur the temporal consistency refers only to the most frequent pattern.

1) NORTH ATLANTIC OSCILLATION

Figure 2ii indicates that there is a significant 40-yr climatological relationship between the NAO and SAT that extends across northern Russia as far east as the Verkhoyanskiy Mountains. However, Fig. 7i reveals that the proportion of individual decades for which a significant relationship exists is considerably less than the maximum possible across the majority of this region. The most consistent significant decadal impact of the NAO on SAT is observed in the Northern European Plain, where the temporal consistency is ~75%. Indeed, there is a small area where the NAO significantly impacts SAT in more than 90% of decades (i.e., where the relationship is essentially temporally invariant). The temporal consistency generally decreases rapidly to the north and especially east, although there are regions, such as the Kola Peninsula and West Siberian Plateau, where it exceeds 60%. The equivalent plot for PPN (Fig. 7ii) indicates that the spatial extent where the NAO–PPN temporal consistency is at a given level is markedly smaller than for NAO and SAT: the only regions where the temporal consistency is more than 60% are the southern Kola Peninsula and a small part of Karelia. With a few exceptions, such as the Taymyr Peninsula, areas where the NAO–PPN relationship has a temporal consistency greater than 30% only extend as far east as ~45°E.

2) EAST ATLANTIC

Despite the significant EA–SAT climatological relationship between 45° and 120°E (Fig. 2v), there are very few terrestrial areas where the temporal consistency of the relationship exceeds 30% (Fig. 7iii). Interestingly, there is not a single decade in 1980–2019 when there is a significant relationship between EA and SAT across the majority of the North European Plain and West Siberian Plateau. There are similarly few areas of northern Russia where a significant EA–PPN relationship occurs in more than 30% of decades (Fig. 7iv). They include a spatially coherent region in the West Siberian Plateau south of ~62°N, while smaller areas encompass Zemlya Frantsa Iosifa and Severnaya Zemlya.

3) WEST PACIFIC

The WP has the most consistent significant impact on SAT in the mountainous regions of Far East Siberia. Here, the

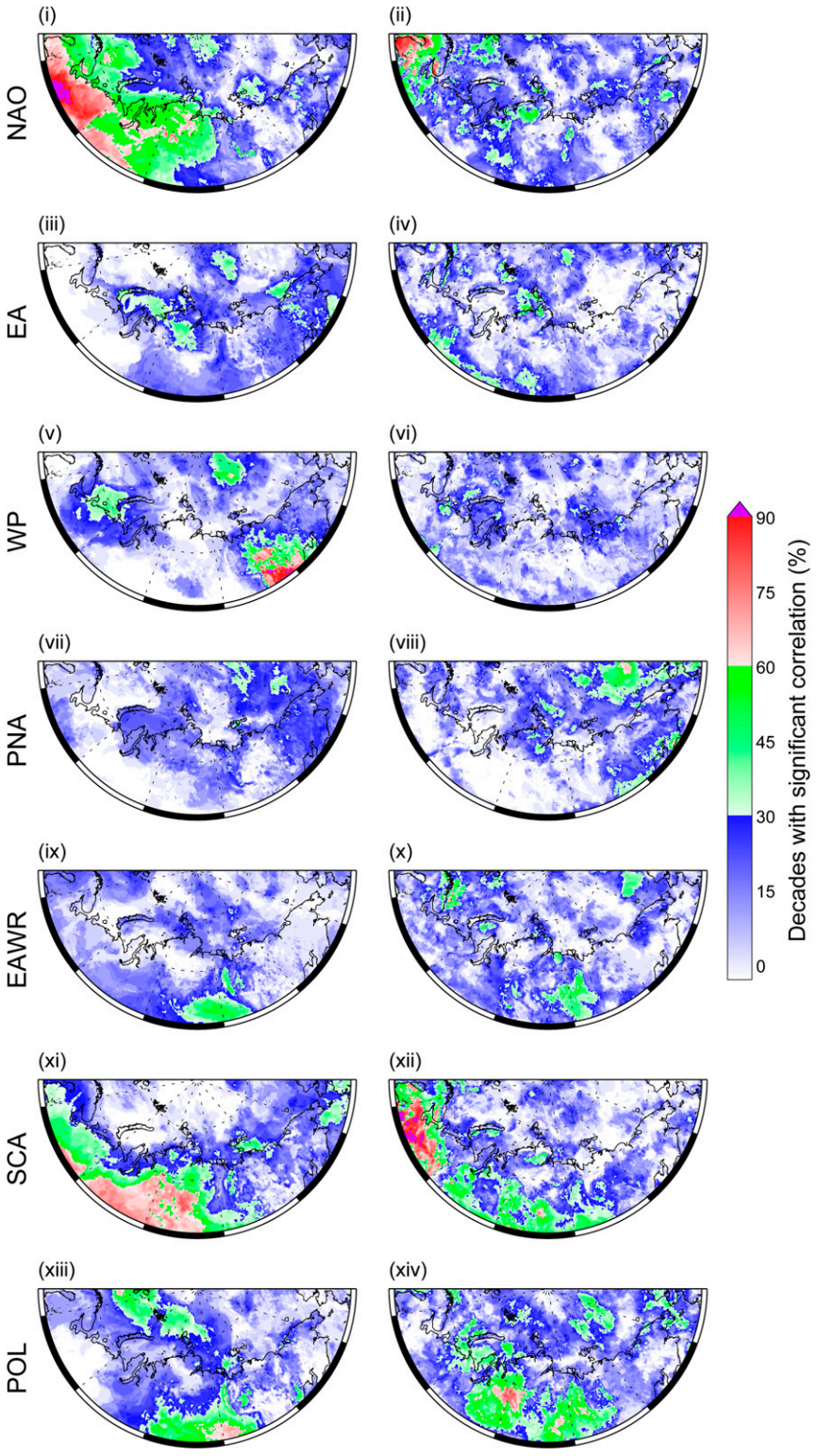

FIG. 7. The temporal consistency of significant winter decadal relationships ($p < 0.10$) between the circulation patterns and (left) SAT and (right) PPN based on ERA5 data for 1980–2019.

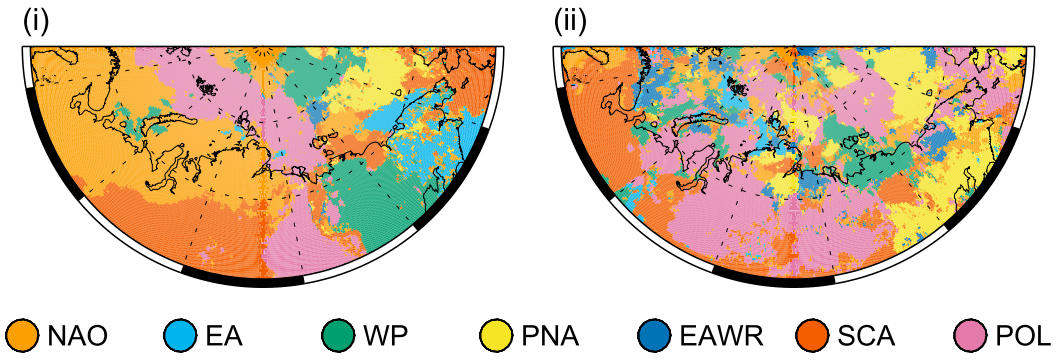

FIG. 8. The circulation pattern exerting the most consistent significant winter decadal impact (see text for definition) on (left) SAT and (right) PPN.

temporal consistency generally exceeds 30%, and increases to more than 60% in some areas (Fig. 7v). Interestingly, a significant decadal relationship between the WP and SAT is also observed in the Barents Sea region during more than 30% of the period examined. In contrast, there are very few decades when WP has any significant impact on PPN in Far East Siberia or indeed across the whole of northern Russia (Fig. 7vi).

4) PACIFIC–NORTH AMERICA

There are no areas of northern Russia where the relationship between the PNA pattern and SAT has a temporal consistency of more than 30% (Fig. 7vii), not unexpected given the climatology (Fig. 2xi). Unsurprisingly, the areas with the most consistent PNA impact on SAT are found in Far East Siberia, the region closest to the PNA center of action in the North Pacific. The land areas where the PNA–PPN relationship is significant in more than 30% of decades are limited to parts of Far East Siberia south of ~61°N and the Taymyr Peninsula (Fig. 7viii).

5) EAST ATLANTIC/WESTERN RUSSIA

The primary region where significant relationships between the EAWR pattern and both SAT and PPN have a temporal consistency greater than 30% is the eastern side of the Central Siberian Plateau at ~120°E (cf. Figs. 7ix and 7x). In addition, the EAWR has a significant decadal relationship with PPN in the northern Kola Peninsula for more than 30% of the time.

6) SCANDINAVIAN

The extent of northern Russia where the temporal consistency between the SCA and SAT is greater than 30% aligns approximately with that where there is a significant climatological relationship (cf. Figs. 7xi and 2xvii), an observation that applies to other patterns too. However, across the majority of this region the temporal consistency is more than 60%, predominantly in the West Siberian Plains and Central Siberia Plateau. In the latter region the SCA–SAT relationship is more temporally consistent than NAO–SAT. Regarding PPN, Fig. 7xii indicates that the area where the temporal consistency exceeds 60% is shifted west relative to SAT and in parts of the North European Plain the SCA–PPN relationship is temporally invariant. Similar to the climatology, at a given latitude of the North European Plain the temporal consistency of the SCA–PPN relationship is generally greater than for SCA–SAT (Figs. 7xi and xii).

7) POLAR/EURASIA

The temporal consistency of winter decadal POL–SAT and POL–PPN relationships in northern Russia are shown in Figs. 7xiii and 7xiv, respectively. For SAT, areas with a temporal consistency of 30% comprise the Central Siberian Plateau south of ~65°N, while for PPN they consist of the western and eastern flanks of the same region but with reduced temporal consistency in the center. For both parameters there are small areas where the proportion of decades with a significant relationship with POL is greater than 60%. Significant decadal relationships between POL and SAT and/or PPN that have a temporal consistency exceeding 30% are also observed over some Arctic island archipelagos.

Next, we determine the ''dominant'' circulation pattern, defined as having the highest temporal consistency in a region, and examine how that varies spatially across northern Russia. Figure 8i reveals that the NAO is the dominant pattern affecting winter SAT west of the Urals, and also in some Arctic coastal areas to the east, including the Yamal and Taymyr Peninsulas, and over the Barents and Kara Seas and Novaya Zemlya. Farther east, as far as ~110°E, the SCA is generally the dominant pattern, including over much of the Central Siberian Plateau. Immediately to the east of this area and south of ~64°N, the POL becomes dominant, and is also the most temporally consistent pattern affecting SAT over the Laptev Sea and both Zemlya Frantsa Iosifa and Sevenaya Zemlya. In the mountainous regions of Far East Siberia the WP is dominant. While Fig. 7 indicates that no circulation pattern has a temporal consistency exceeding 30% in the farthest east region of northern Russia, it is actually the Atlantic-focused EA pattern that is the dominant pattern affecting SAT there. Moreover, Fig. 8i demonstrates that there are no spatially coherent areas where either the PNA or EAWR is the dominant pattern influencing SAT in northern Russia.

The spatial distribution of the dominant circulation pattern influencing winter PPN is shown in Fig. 8ii. In general, it is less clearly defined than for SAT, especially over the ocean and Arctic islands, but there are still distinct spatial patterns. The

SCA is dominant across the Kola Peninsula, Karelia, and the Northern European Plain, together with smaller areas of the West Siberian Plains and Central Siberian Plateau and even as far east as the Chersky Mountains. However, Fig. 8ii reveals that POL is clearly the dominant pattern affecting PPN across the significant majority of both the West Siberian Plains and Central Siberian Plateau. In Far East Siberia there is more of a latitudinal variation in the dominant pattern. Between 60° and 65°N the PNA is dominant while farther north it is the SCA, WP, and EAWR, although these latter three all have a temporal consistency less than 30% here. There are no significant areas of northern Russia where either the NAO or EA is the dominant pattern affecting PPN (cf. Fig. 8ii).

The most extreme response of the observed marked decadal variability in the impact of atmospheric circulation patterns is when statistically significant relationships of both signs arise. While such areas do exist, being most prevalent in Far East Siberia, a false discovery rate test (e.g., Wilks 2006) reveals that the significant majority probably arise through chance.

d. Extending the length of the analysis

One shortcoming of using ERA5 for this analysis is that 40 years is a relatively short time period over which to examine decadal variability. Given that the CPC indices of the atmospheric circulation patterns begin in 1950, there is the potential to use the JRA-55, for which data are available from 1958 to the present, to extend the length of the analysis to 61 years and hence determine whether our findings remain valid over this longer time period. Figure S4 shows the temporal consistency of the significant decadal relationships between the seven circulation patterns and SAT and PPN based on JRA-55 data, for the 1980–2019 overlap period with ERA5. The two reanalyses are generally very similar, with no fundamental differences, indicating that the ERA5 results are robust. The regions of high temporal consistency (>60%) tend to be more spatially coherent in JRA-55, likely due to the poorer spatial resolution of this reanalysis. This means that some local details are missed, such as the clear change in temporal consistency between the POL pattern and SAT associated with the Verhoyansk Mountains seen in the ERA5 data (cf. Fig. 7xiii and Fig. S4xiii). However, overall the two reanalyses are sufficiently similar to justify using the JRA-55 as a direct comparison in order to increase the length of the analysis.

Plots of the winter decadal temporal consistency between the circulation patterns and SAT and PPN based on 61 years of the JRA-55 from 1959 to 2019 are shown in Fig. 9. There are no major disparities between this figure and that for the shorter ERA5-based analysis (Fig. 7). Nonetheless, there are a few noteworthy differences. For example, the JRA-55 data reveal reduced temporal consistency between the NAO and SAT over the Northern European Plain and West Siberian Plains, although it increases over the Yamal Peninsula (cf. Figs. 7i and 9i). Conversely, the temporal consistency between the NAO and PPN in these regions is generally greater in the longer time series (cf. Figs. 7ii and 9ii). This is also true of the SCA relationships with climate: in particular there is a clear reduction (increase) in temporal consistency between the SCA and SAT (PPN) over the West Siberian Plains (cf. Figs. 7xi,xii and 9xi,xii). The region in the mountains of Far East Siberia where the temporal consistency between the WP and SAT is more than 30% is expanded in the JRA-55 data and now reaches >90%, but the higher consistency in the Barents Sea has disappeared (cf. Figs. 7v and 9v). The longer time series also demonstrates reductions in the extent of regions where the temporal consistency of both POL–SAT and POL–PPN is greater than 30%. In contrast, the temporal consistency of regional climate relationships with the EA, PNA, and EAWR is generally slightly higher in the JRA-55 data but there remain relatively few areas that exceed 30%.

4. Discussion and conclusions

In this paper we have investigated the decadal variability of the impact of seven atmospheric circulation patterns on the winter climate of northern Russia, as represented by SAT and PPN. Our results provide a measure against which climate model output for recent decades can be assessed (e.g., Gong et al. 2017), and future projections compared and estimates of their uncertainty improved.

The analysis, based on 40 years of ERA5 data, has demonstrated that there is indeed marked decadal variability in the spatial locations and extent of northern Russia over which these patterns exert a statistically significant influence on climate, often concomitant with long-term significant relationships. Examination of four consecutive decades established that some of this variability is a direct response to the changing location of a pattern's center(s) of action, which affects the spatial distribution of advection of heat and moisture into and across the region. These changes are likely a response to both natural variability within the climate system and external anthropogenic forcing (e.g., Dong et al. 2010; L. Wang et al. 2019). The temporal consistency of significant winter decadal relationships between each circulation pattern and SAT or PPN was determined by analyzing each of the 31 decades contained within the 40-yr study period. Regions of northern Russia with climatological, statistically significant relationships between atmospheric circulation patterns and climate approximately match those with a decadal temporal consistency of only 30%, and thus the climatology masks considerable decadal variability. Extending the period examined from 40 to 61 years using JRA-55 did not significantly alter any of our conclusions, although there are limited expansions and/or contractions of areas with higher temporal consistency for some circulation pattern–climate relationships. Our principal findings regarding each of the atmospheric circulation patterns are as follows:

- The NAO is the dominant pattern (has the highest winter decadal temporal consistency) affecting SAT across northern Russia west of the Urals, and also some Arctic coastal areas farther east. Regions with a high (>60%) temporal consistency between the NAO and PPN are limited to the southern Kola Peninsula and parts of Karelia.
- Of the atmospheric circulation patterns studied, the EA generally has the least consistent decadal impact on the winter climate of northern Russia, despite some regions having a significant climatological connection with SAT or PPN.
- The WP has its most consistent impact on winter SAT in the mountainous regions of Far East Siberia, where it is the dominant pattern examined. In contrast, there are very few

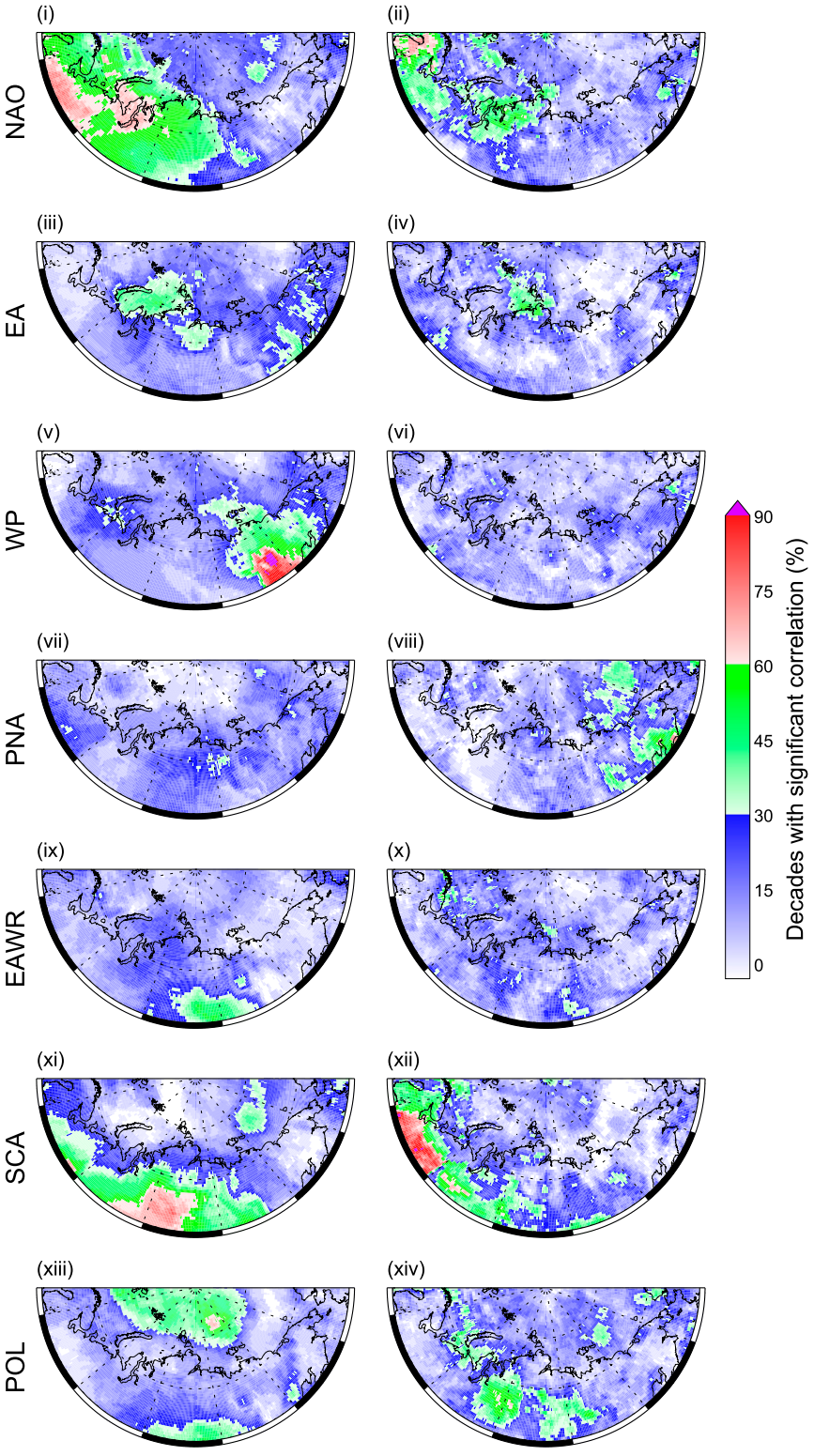

FIG. 9. As in Fig. 7, but based on JRA-55 data for 1959–2019.

decades when WP has any significant impact on winter PPN anywhere in northern Russia.
- Similarly, there are few decades when the PNA pattern has a significant influence on winter SAT in northern Russia. Unsurprisingly, the area with the most consistent decadal PNA impact on winter PPN is found in Far East Siberia.
- The EAWR pattern has its primary impact on climate on the eastern side of the Central Siberian Plateau, where the temporal consistency of the relationship with both SAT and PPN is greater than 30%.
- A high temporal consistency of the winter SCA–SAT relationship occurs in some areas of the West Siberian Plains and Central Siberian Plateau. In the former region the SCA is the dominant pattern affecting SAT. The equivalent region for winter SCA–PPN is shifted west relative to SAT, and in parts of the North European Plain the relationship is temporally invariant. The SCA is the dominant pattern influencing PPN there, and also in the Kola Peninsula, Karelia, and smaller areas farther east.
- POL is the dominant pattern affecting both winter SAT and PPN in much of the Central Siberian Plateau region and also PPN over the West Siberian Plains.

In this study we have examined the changes in decadal impact of each atmospheric circulation pattern in isolation. However, a small number of studies have investigated the changing locations of the north–south dipole of the NAO and shown that its interplay with the EA and SCA patterns exerts one of the primary controls governing the position of its centers of action (Moore et al. 2013; Comas-Bru and McDermott 2014; Mellado-Cano et al. 2019) and subsequent impacts on, for example, the carbon cycle (Bastos et al. 2016) and precipitation (Álvarez-García et al. 2019). Based on the CPC sign conventions used in the present study, when the NAO and EA are of the same sign there is a southwest movement in the centers of action while when the NAO and SCA are of the same sign there is a counterclockwise rotation of the centers (and vice versa). If we examine the 1980s as an example, during this decade the most frequent winter NAO–EA combination was positive NAO and negative EA and similarly the most frequent NAO–SCA combination was positive NAO and negative SCA. According to the two premises above, the northerly NAO center of action should have been negative and shifted both to the northeast movement and rotated clockwise relative to its climatological position. Comparing Figs. 2i and 5i indicates that this is indeed the case in the 1980s. The other three successive decades also follow the premises reasonably well, with the NAO–EA interplay appearing to have a greater influence than that between the NAO and SCA, possibly due to the inversely weighted contribution to regional SLP variability between the NAO and SCA, as noted by Kislov and Matveeva (2020).

Given that we have established that the magnitude of the eastward extension of the northern NAO center has a major impact on the winter climate of much of northern Russia, such interactions between these and different combinations of circulation patterns are likely to contribute to the overall climate variability of the region, including the persistence of SAT anomalies into the following spring (Chen et al. 2018; Wu and Chen 2020). Therefore, future work will use machine-learning techniques, based on nonlinear regression analysis, to describe the interplay between the various different patterns and to quantify the extent to which it contributes to the marked winter decadal-scale variability in the impact of the individual patterns on northern Russian climate as described in this study.

Acknowledgments. We thank the editor and three reviewers for their positive critiques and suggestions. G.J.M. was supported by the U.K. Natural Environment Research Council (NERC) through the British Antarctic Survey research programme ''Polar Science for Planet Earth.'' The research was undertaken under the auspices of the British–Russian project ''Multiplatform remote sensing of the impact of climate change on the northern forests of Russia,'' funded by the British Council (Grant 352397111) and the Ministry of Science and Higher Education of the Russian Federation (project RFMEFI61618 X0099).

Data availability statement. The monthly ERA5 data were obtained from https://doi.org/10.24381/cds.f17050d7. The monthly JRA-55 data were obtained from https://rda.ucar.edu/datasets/ds628.1. The time series of the seven atmospheric circulation patterns were obtained from https://www.cpc.ncep.noaa.gov/data/teledoc/telecontents.shtml.

REFERENCES

Álvarez-García, F. J., M. J. OrtizBevia, W. Cabos, M. Tasambay-Salazar, and A. Ruiz de Elvira, 2019: Linear and nonlinear links of winter European precipitation to Northern Hemisphere circulation patterns. *Climate Dyn.*, **52**, 6533–6555, https://doi.org/10.1007/s00382-018-4531-6.

Bader, J., M. D. S. Mesquita, K. I. Hodges, N. Keenlyside, S. Østerhus, and M. Miles, 2011: A review on Northern Hemisphere sea-ice, storminess and the North Atlantic Oscillation: Observations and projected changes. *Atmos. Res.*, **101**, 809–834, https://doi.org/10.1016/j.atmosres.2011.04.007.

Barnston, A. G., and R. E. Livezey, 1987: Classification, seasonality and persistence of low-frequency atmospheric circulation patterns. *Mon. Wea. Rev.*, **115**, 1083–1126, https://doi.org/10.1175/1520-0493(1987)115<1083:CSAPOL>2.0.CO;2.

Bastos, A., and Coauthors, 2016: European land CO_2 sink influenced by NAO and East-Atlantic pattern coupling. *Nat. Commun.*, **7**, 10315, https://doi.org/10.1038/ncomms10315.

Box, J. E., and Coauthors, 2019: Key indicators of Arctic climate change: 1971–2017. *Environ. Res. Lett.*, **14**, 045010, https://doi.org/10.1088/1748-9326/aafc1b.

Brown, M. B., and A. B. Forsythe, 1974: Robust tests for the equality of variances. *J. Amer. Stat. Assoc.*, **69**, 364–367, https://doi.org/10.1080/01621459.1974.10482955.

Bueh, C., and H. Nakamura, 2007: Scandinavian pattern and its climatic impact. *Quart. J. Roy. Meteor. Soc.*, **133**, 2117–2131, https://doi.org/10.1002/qj.173.

Casanueva, A., C. Rodríguez-Puebla, M. D. Frías, and N. González-Reviriego, 2014: Variability of extreme precipitation over Europe and its relationships with teleconnection patterns. *Hydrol. Earth Syst. Sci.*, **18**, 709–725, https://doi.org/10.5194/hess-18-709-2014.

Chen, S., and L. Song, 2018: Impact of the winter North Pacific Oscillation on the surface air temperature over Eurasia and

North America: Sensitivity to the index definition. *Adv. Atmos. Sci.*, **35**, 702–712, https://doi.org/10.1007/s00376-017-7111-5.

——, W. Wu, L. Song, and W. Chen, 2018: Combined influence of the Arctic Oscillation and the Scandinavia pattern on spring surface air temperature variations over Eurasia. *J. Geophys. Res. Atmos.*, **123**, 9410–9429, https://doi.org/10.1029/2018JD028685.

——, R. Wu, and W. Chen, 2020: Strengthened connection between springtime North Atlantic Oscillation and North Atlantic tripole SST pattern since the late 1980s. *J. Climate*, **33**, 2007–2022, https://doi.org/10.1175/JCLI-D-19-0628.1.

Chylek, P., N. Hengartner, G. Lesins, J. D. Klett, O. Humlum, M. Wyatt, and M. K. Dubey, 2014: Isolating the anthropogenic component of Arctic warming. *Geophys. Res. Lett.*, **41**, 3569–3576, https://doi.org/10.1002/2014GL060184.

Cohen, J., and Coauthors, 2020: Divergent consensuses on Arctic amplification influence on midlatitude severe winter weather. *Nat. Climate Change*, **10**, 20–29, https://doi.org/10.1038/s41558-019-0662-y.

Comas-Bru, L., and F. McDermott, 2014: Impacts of the EA and SCA patterns on the European twentieth century NAO–winter climate relationship. *Quart. J. Roy. Meteor. Soc.*, **140**, 354–363, https://doi.org/10.1002/qj.2158.

Cooper, E. J., 2014: Warmer shorter winters disrupt Arctic terrestrial ecosystems. *Annu. Rev. Ecol. Evol. Syst.*, **45**, 271–295, https://doi.org/10.1146/annurev-ecolsys-120213-091620.

Crasemann, B., D. Handorf, R. Jaiser, K. Dethloff, T. Nakamura, J. Ukita, and K. Yamazaki, 2017: Can preferred atmospheric circulation patterns over the North Atlantic-Eurasian region be associated with Arctic sea ice loss? *Polar Sci.*, **14**, 9–20, https://doi.org/10.1016/j.polar.2017.09.002.

Degirmendžić, J., and K. Kożuchowski, 2019: Variation of macrocirculation forms over the Atlantic-Eurasian temperate zone according to the Vangengeim-Girs classification. *Int. J. Climatol.*, **39**, 4938–4952, https://doi.org/10.1002/joc.6118.

Dong, B., R. T. Sutton, and T. Woollings, 2010: Changes of interannual NAO variability in response to greenhouse gases forcing. *Climate Dyn.*, **37**, 1621–1641, https://doi.org/10.1007/s00382-010-0936-6.

Feldstein, S. B., 2002: The recent trend and variance increase of the annular mode. *J. Climate*, **15**, 88–94, https://doi.org/10.1175/1520-0442(2002)015<0088:TRTAVI>2.0.CO;2.

Forbes, B. C., and Coauthors, 2016: Sea ice, rain-on-snow and tundra reindeer nomadism in Arctic Russia. *Biol. Lett.*, **12**, 20160466, https://doi.org/10.1098/rsbl.2016.0466.

Franzke, C., and S. B. Feldstein, 2005: The continuum and dynamics of Northern Hemisphere teleconnection patterns. *J. Atmos. Sci.*, **62**, 3250–3267, https://doi.org/10.1175/JAS3536.1.

Frey, K. E., and L. C. Smith, 2003: Recent temperature and precipitation increases in West Siberia and their association with the Arctic Oscillation. *Polar Res.*, **22**, 287–300, https://doi.org/10.3402/polar.v22i2.6461.

Gao, T., J.-Y. Yu, and H. Paek, 2016: Impacts of four Northern-Hemisphere teleconnection patterns on atmospheric circulations over Eurasia and the Pacific. *Theor. Appl. Climatol.*, **129**, 815–831, https://doi.org/10.1007/s00704-016-1801-2.

Gong, H., L. Wang, W. Chen, X. Chen, and D. Nath, 2017: Biases of the wintertime Arctic Oscillation in CMIP5 models. *Environ. Res. Lett.*, **12**, 014001, https://doi.org/10.1088/1748-9326/12/1/014001.

Goosse, K., and M. M. Holland, 2005: Mechanisms of decadal Arctic climate variability in the Community Climate System Model, version 2 (CCSM2). *J. Climate*, **18**, 3552–3570, https://doi.org/10.1175/JCLI3476.1.

Groisman, P., and Coauthors, 2017: Northern Eurasia Future Initiative (NEFI): Facing the challenges and pathways of global change in the twenty-first century. *Prog. Earth Planet. Sci.*, **4**, 41, https://doi.org/10.1186/s40645-017-0154-5.

Handorf, D., and K. Dethloff, 2012: How well do state-of-the-art atmosphere–ocean general circulation models reproduce atmospheric teleconnection patterns? *Tellus*, **64A**, 19777, https://doi.org/10.3402/tellusa.v64i0.19777.

Hanna, E., T. E. Cropper, P. D. Jones, A. A. Scaife, and R. Allan, 2015: Recent seasonal asymmetric changes in the NAO (a marked summer decline and increased winter variability) and associated changes in the AO and Greenland Blocking Index. *Int. J. Climatol.*, **35**, 2540–2554, https://doi.org/10.1002/joc.4157.

Henderson, G. R., Y. Peings, J. C. Furtado, and P. J. Kushner, 2018: Snow–atmosphere coupling in the Northern Hemisphere. *Nat. Climate Change*, **8**, 954–963, https://doi.org/10.1038/s41558-018-0295-6.

Hersbach, H., and Coauthors, 2020: The ERA5 global reanalysis. *Quart. J. Roy. Meteor. Soc.*, **146**, 1999–2049, https://doi.org/10.1002/qj.3803.

Hoy, A., M. Sepp, and J. Matschullat, 2013: Large-scale atmospheric circulation forms and their impact on air temperature in Europe and northern Asia. *Theor. Appl. Climatol.*, **113**, 643–658, https://doi.org/10.1007/s00704-012-0813-9.

Hurrell, J. W., 1995: Decadal trends in the North Atlantic Oscillation: Regional temperatures and precipitation. *Science*, **269**, 676–679, https://doi.org/10.1126/science.269.5224.676.

——, Y. Kushnir, G. Ottersen, and M. Visbeck, 2003: An overview of the North Atlantic Oscillation. *The North Atlantic Oscillation: Climatic Significance and Environmental Impact*, *Geophys. Monogr.*, Vol. 134, Amer. Geophys. Union, 1–37.

Ionita, M., 2014: The impact of the east Atlantic/western Russia pattern on the hydroclimatology of Europe from mid-winter to late spring. *Climate*, **2**, 296–309, https://doi.org/10.3390/cli2040296.

Kalnay, E., and Coauthors, 1996: The NCEP/NCAR 40-Year Reanalysis Project. *Bull. Amer. Meteor. Soc.*, **77**, 437–472, https://doi.org/10.1175/1520-0477(1996)077<0437:TNYRP>2.0.CO;2.

Kislov, A., and T. Matveeva, 2020: The monsoon over the Barents Sea and Kara Sea. *Atmos. Climate Sci.*, **10**, 339–356, https://doi.org/10.4236/acs.2020.103019.

Kobayashi, S., and Coauthors, 2015: The JRA-55 reanalysis: General specifications and basic characteristics. *J. Meteor. Soc. Japan*, **93**, 5–48, https://doi.org/10.2151/jmsj.2015-001.

Kolstad, E. W., and J. A. Screen, 2019: Nonstationary relationship between autumn Arctic sea ice and the winter North Atlantic Oscillation. *Geophys. Res. Lett.*, **46**, 7583–7591, https://doi.org/10.1029/2019GL083059.

Kryjov, V. N., 2015: October circulation precursors of the wintertime Arctic Oscillation. *Int. J. Climatol.*, **35**, 161–171, https://doi.org/10.1002/joc.3968.

Lim, Y.-K., 2015: The East Atlantic/West Russia (EA/WR) teleconnection in the North Atlantic: Climate impact and relation to Rossby wave propagation. *Climate Dyn.*, **44**, 3211–3222, https://doi.org/10.1007/s00382-014-2381-4.

Linkin, M. E., and S. Nigam, 2008: The North Pacific Oscillation–west Pacific teleconnection pattern: Mature-phase structure and winter impacts. *J. Climate*, **21**, 1979–1997, https://doi.org/10.1175/2007JCLI2048.1.

Liu, Y., L. Wang, W. Zhou, and W. Chen, 2014: Three Eurasian teleconnection patterns: Spatial structures, temporal variability, and associated winter climate anomalies. *Climate Dyn.*, **42**, 2817–2839, https://doi.org/10.1007/s00382-014-2163-z.

Marshall, G. J., R. M. Vignols, and W. G. Rees, 2016: Climate change in the Kola Peninsula, Arctic Russia, during the last 50 years from meteorological observations. *J. Climate*, **29**, 6823–6840, https://doi.org/10.1175/JCLI-D-16-0179.1.

——, S. Kivinen, K. Jylhä, R. M. Vignols, and W. G. Rees, 2018: The accuracy of climate variability and trends across Arctic Fennoscandia in four reanalyses. *Int. J. Climatol.*, **38**, 3878–3895, https://doi.org/10.1002/joc.5541.

——, K. Jylhä, S. Kivinen, M. Laapas, and A. V. Dyrrdal, 2020: The role of atmospheric circulation patterns in driving recent changes in indices of extreme seasonal precipitation across Arctic Fennoscandia. *Climatic Change*, **162**, 741–759, https://doi.org/10.1007/s10584-020-02747-w.

Mellado-Cano, J., D. Barriopedro, R. García-Herrera, R. M. Trigo, and A. Hernández, 2019: Examining the North Atlantic Oscillation, east Atlantic pattern, and jet variability since 1685. *J. Climate*, **32**, 6285–6298, https://doi.org/10.1175/JCLI-D-19-0135.1.

Min, S. K., X. Zhang, and F. Zwiers, 2008: Human-induced Arctic moistening. *Science*, **320**, 518–520, https://doi.org/10.1126/science.1153468.

Moore, G. W. K., I. A. Renfrew, and R. S. Pickart, 2013: Multidecadal mobility of the North Atlantic Oscillation. *J. Climate*, **26**, 2453–2466, https://doi.org/10.1175/JCLI-D-12-00023.1.

Overland, J. E., and Coauthors, 2016: Nonlinear response of mid-latitude weather to the changing Arctic. *Nat. Climate Change*, **6**, 992–999, https://doi.org/10.1038/nclimate3121.

Peings, Y., 2019: Ural blocking as a driver of early-winter stratospheric warmings. *Geophys. Res. Lett.*, **46**, 5460–5468, https://doi.org/10.1029/2019GL082097.

Pokorná, L., and R. Huth, 2015: Climate impacts of the NAO are sensitive to how the NAO is defined. *Theor. Appl. Climatol.*, **119**, 639–652, https://doi.org/10.1007/s00704-014-1116-0.

Popova, V., 2007: Winter snow depth variability over northern Eurasia in relation to recent atmospheric circulation changes. *Int. J. Climatol.*, **27**, 1721–1733, https://doi.org/10.1002/joc.1489.

——, 2018: Present-day changes in climate in the north of Eurasia as a manifestation of variation of the large-scale atmospheric circulation (in Russian). *Fund. Appl. Climatol.*, **1**, 84–111, https://doi.org/10.21513/2410-8758-2018-1-84-111.

Shmakin, A. B., and V. V. Popova, 2006: Dynamics of climate extremes in northern Eurasia in the late 20th century. *Izv. Atmos. Oceanic Phys.*, **42**, 138–147, https://doi.org/10.1134/S0001433806020022.

Thompson, D. W. J., and J. M. Wallace, 1998: The Arctic Oscillation signature in the wintertime geopotential height and temperature fields. *Geophys. Res. Lett.*, **25**, 1297–1300, https://doi.org/10.1029/98GL00950.

van der Linden, E. C., R. Bintanja, and W. Hazeleger, 2017: Arctic decadal variability in a warming world. *J. Geophys. Res.*, **122**, 5677–5696, https://doi.org/10.1002/2016JD026058.

Vasiliev, A. A., S. S. Drozdov, A. G. Gravis, G. V. Malkova, K. E. Nyland, and D. A. Streletskiy, 2020: Permafrost degradation in the western Russia Arctic. *Environ. Res. Lett.*, **15**, 045001, https://doi.org/10.1088/1748-9326/ab6f12.

Vicente-Serrano, S. M., and J. I. López-Moreno, 2008: Nonstationary influence of the North Atlantic Oscillation on European precipitation. *J. Geophys. Res.*, **113**, D20120, https://doi.org/10.1029/2008JD010382.

Wallace, J. M., and D. S. Gutzler, 1981: Teleconnections in the geopotential height field during the Northern Hemisphere winter. *Mon. Wea. Rev.*, **109**, 784–812, https://doi.org/10.1175/1520-0493(1981)109<0784:TITGHF>2.0.CO;2.

Wang, C., R. M. Graham, K. Wang, S. Gerland, and M. A. Granskog, 2019: Comparison of ERA5 and ERA-Interim near-surface air temperature, snowfall and precipitation over Arctic sea ice: Effects on sea ice thermodynamics and evolution. *Cryosphere*, **13**, 1661–1679, https://doi.org/10.5194/tc-13-1661-2019.

Wang, L., Y. Liu, Y. Zhang, W. Chen, and S. Chen, 2019: Time-varying structure of the wintertime Eurasian pattern: Role of the North Atlantic sea surface temperature and atmospheric mean flow. *Climate Dyn.*, **52**, 2467–2479, https://doi.org/10.1007/s00382-018-4261-9.

Wilks, D. S., 2006: On "field significance" and the false discovery rate. *J. Appl. Meteor. Climatol.*, **45**, 1181–1191, https://doi.org/10.1175/JAM2404.1.

World Weather Attribution, 2020: Prolonged Siberian heat of 2020. Accessed 16 July 2020, https://www.worldweatherattribution.org/wp-content/uploads/WWA-Prolonged-heat-Siberia-2020.pdf.

Wu, B., D. Handorf, K. Dethloff, A. Rinke, and A. Hu, 2013: Winter weather patterns over northern Eurasia and Arctic sea ice loss. *Mon. Wea. Rev.*, **141**, 3786–3800, https://doi.org/10.1175/MWR-D-13-00046.1.

Wu, R., and S. Chen, 2020: What leads to persisting surface air temperature anomalies from winter to following spring over mid- to high-latitude Eurasia? *J. Climate*, **33**, 5861–5883, https://doi.org/10.1175/JCLI-D-19-0819.1.

Ye, K., R. Wu, and Y. Liu, 2015: Interdecadal change of Eurasian snow, surface temperature, and atmospheric circulation in the late 1980s. *J. Geophys. Res. Atmos.*, **120**, 2738–2753, https://doi.org/10.1002/2015JD023148.

Yu, L., C. Sui, D. H. Lenschow, and M. Zhou, 2017: The relationship between wintertime extreme temperature events north of 60°N and large-scale atmospheric circulations. *Int. J. Climatol.*, **37**, 597–611, https://doi.org/10.1002/joc.5024.

Zhang, X., A. Sorteberg, J. Zhang, R. Gerdes, and J. C. Comiso, 2008: Recent radical shifts of atmospheric circulations and rapid changes in Arctic climate system. *Geophys. Res. Lett.*, **35**, L22701, https://doi.org/10.1029/2008GL035607.